Probability Distribution of Peaks for Nonlinear Combination of Vector Gaussian Loads

Sayan Gupta[1]
Assistant Professor
Department of Applied Mechanics,
Indian Institute of Technology Madras,
Chennai 600036, India
e-mail: s.gupta@tudelft.nl

P. H. A. J. M. van Gelder
Associate Professor
e-mail: p.h.a.j.m.vangelder@tudelft.nl

Department of Civil Engineering,
Technical University of Delft,
Stevinweg 1,
P.O. Box 5048,
2600 GA Delft, The Netherlands

The problem of approximating the probability distribution of peaks, associated with a special class of non-Gaussian random processes, is considered. The non-Gaussian processes are obtained as nonlinear combinations of a vector of mutually correlated, stationary, Gaussian random processes. The Von Mises stress in a linear vibrating structure under stationary Gaussian loadings is a typical example for such processes. The crux of the formulation lies in developing analytical approximations for the joint probability density function of the non-Gaussian process and its instantaneous first and second time derivatives. Depending on the nature of the problem, this requires the evaluation of a multidimensional integration across a possibly irregular and disjointed domain. A numerical algorithm, based on first order reliability method, is developed to evaluate these integrals. The approximations for the peak distributions have applications in predicting the expected fatigue damage due to combination of stress resultants in a randomly vibrating structure. The proposed method is illustrated through two numerical examples and its accuracy is examined with respect to estimates from full scale Monte Carlo simulations of the non-Gaussian process. [DOI: 10.1115/1.2890404]

Keywords: random vibrations, peak distributions, non-Gaussian process, vector Gaussian processes, nonlinear combination, expected fatigue damage

1 Introduction

The study of properties of random processes constitutes an important aspect of time variant structural reliability analysis. For structures under randomly vibrating loads, the structure response is a random process. Estimates on the safety of such structures are made by studying properties of these response processes, such as the number of level crossings in a given time interval, the fraction of time spent above specified threshold levels, the first passage times, the extreme value distributions and the probability distribution of the peaks [1]. Of these properties, the latter is of particular interest in estimating the fatigue damage in randomly vibrating structures [2,3]. This, in turn, is of use in predicting the lifetime of existing structures.

As in many areas of random vibration, estimates of the expected fatigue damage may be obtained via the Monte Carlo method. It is well established that the Monte Carlo method offers the best accuracy subject to the limitations of the size of the samples considered in the analysis. However, high computational costs and large data storage requirements often prove to be major limitations in implementation of this technique. This is particularly true in fatigue analysis, which usually involves analysis of long time histories. On the other hand, analytical methods, though often built on certain assumptions, provide elegant and easy to compute solutions, which have acceptable levels of accuracy.

In this study, we employ the peak-counting method, which is one of the simplest fatigue damage estimation techniques available in the literature. The underlying principle of this method lies in the assumption that fatigue damage occurs due to stress reversals, which, in turn, are associated with peaks in the structure response time history. In the time domain analysis, this involves counting the number of peaks, corresponding to various stress levels, and estimating the fatigue damage corresponding to each such peak. The total fatigue damage is obtained as a summation of all such incremental damages. For random time histories, the total fatigue damage is a random variable, for which the mean fatigue damage is the simplest descriptor for the random fatigue. Estimating the mean fatigue damage corresponding to the peak-counting method, using analytical methods, requires the knowledge of the probability density function (pdf) of the peaks for the structure response, modeled as a random process. This knowledge is, however, seldom available and is limited to certain classes of loadings.

The focus of this paper is on developing analytical approximations for the peak distributions for non-Gaussian loads, obtained as nonlinear combinations of a vector of stationary Gaussian loads. This, in turn, implies that one needs to develop approximations for the joint pdf's for the non-Gaussian process, its first and second time derivatives, at a given time instant. This information is available in explicit form for Gaussian random processes and expressions for their peak pdf are available in standard random vibration textbooks [1,3,4]. On the other hand, for loads obtained as nonlinear combination of Gaussian loads, even the marginal pdf of the process is rarely available in explicit form. For a limited class of non-Gaussian processes, a mathematical formulation has been proposed in Ref. [5] for obtaining closed form expressions for the joint pdf for the process and its instantaneous time derivative. Based on this formulation, the present authors have developed a strategy, which enables approximating the joint pdf of the process and its instantaneous time derivative, for a wider class of non-Gaussian processes obtained as a nonlinear combination of vector Gaussian processes [6]. The formulations developed in Refs. [5,6] are of use in estimating the probability of first passage failures.

In this paper, we extend the formulation to develop approximation for the joint pdf of similar non-Gaussian processes and their first and second time derivatives. This, in turn, leads to an approximation for the pdf of the peaks for the non-Gaussian process. The approximations for the peak pdf are of use in estimating the expected fatigue damage due to multiaxial loads in randomly vibrating structures.

[1]Corresponding author.

Contributed by the Technical Committee on Vibration and Sound of ASME for publication in the JOURNAL OF VIBRATION AND ACOUSTICS. Manuscript received July 14, 2006; final manuscript received January 31, 2007; published online April 8, 2008. Assoc. Editor: Sotirios Natsiavas.

2 Formulation

We consider a class of non-Gaussian random processes, $V(t)$, which are obtained as nonlinear combinations or transformations, of scalar/vector stationary Gaussian random processes $\{X_j\}_{j=1}^n$. Thus, we represent $V(t)$ as

$$V(t) = g[X_1(t), \ldots, X_n(t)] \tag{1}$$

where, typically, $g[\cdot]$ is a deterministic, nonmonotonic function. As is well known, the occurrence of a peak, at time t, over a threshold v, can be mathematically represented as

$$V(t) \geqslant v$$

$$\dot{V}(t) = 0$$

$$\ddot{V} < 0 \tag{2}$$

Thus, the probability distribution function (PDF) for peaks of $V(t)$ above a threshold level v is dependent on the instantaneous joint pdf of $V(t)$, $\dot{V}(t)$ and $\ddot{V}(t)$. Expressions for the PDF of peaks have been developed in the literature (see Refs. [1,3] for a review) and are given by

$$P_{p_v}(v;t) = 1 - P[p_V \leqslant v] = 1 - \frac{1}{\psi}\int_v^\infty \int_{-\infty}^0 |\ddot{v}| p_{V\dot{V}\ddot{V}}(v,0,\ddot{v};t)\mathrm{d}\ddot{v}\mathrm{d}v \tag{3}$$

where p_V are random variables denoting the peaks of the random process $V(t)$,

$$\psi = \int_{-\infty}^0 |\ddot{v}| p_{\dot{V}\ddot{V}}(0,\ddot{v};t)\mathrm{d}\ddot{v} \tag{4}$$

and $p_{V\dot{V}\ddot{V}}(\cdot)$ is the instantaneous joint pdf for the process $V(t)$ and its first and second time derivatives, denoted by $\dot{V}(t)$ and $\ddot{V}(t)$, respectively. The corresponding pdf for the distribution of peaks of $V(t)$ is given by

$$p_{p_v}(v;t) = \frac{\partial P_{p_v}(v;t)}{\partial v} = \frac{1}{\psi}\int_{-\infty}^0 |\ddot{v}| p_{V\dot{V}\ddot{V}}(v,0,\ddot{v};t)\mathrm{d}\ddot{v} \tag{5}$$

As is evident from Eqs. (3)–(5), a crucial aspect in evaluation of these integrals lies in the fact that the joint pdf $p_{V\dot{V}\ddot{V}}(\cdot)$ should be available. However, in general, when $V(t)$ is non-Gaussian, information on the marginal pdf $p_V(v)$ or the joint pdf $p_{V\dot{V}\ddot{V}}(v,\dot{v},\ddot{v})$ is seldom available.

The crux of the present study, therefore, lies in developing approximations for the joint pdf $p_{V\dot{V}\ddot{V}}(v,0,\ddot{v})$, which, in turn, leads to an approximation for the peak density and distribution functions for non-Gaussian processes of the type shown in Eq. (1). In developing the formulation, we first consider the simple case when $V(t)$ is obtained as a nonmonotonic transformation of a scalar stationary, Gaussian process. Subsequently, we extend the formulation to the case where $\{X_j\}_{j=1}^n$ constitutes a n-dimensional vector of mutually correlated, stationary Gaussian random processes in Sec. 2.2.

2.1 Scalar Case. We consider a stationary non-Gaussian random process $V(t)$, obtained as a nonmonotonic transformation of stationary Gaussian process $X(t)$, such that,

$$V(t) = g[X(t)]$$

$$\dot{V}(t) = g'\dot{X}(t)$$

$$\ddot{V}(t) = g''\dot{X}^2(t) + g'\ddot{X}(t) \tag{6}$$

Here, g' and g'', respectively, denote the first and second derivatives of $g[\cdot]$ with respect to X, at time t. The joint pdf $p_{V\dot{V}\ddot{V}}(\cdot)$ can be expressed in terms of the joint pdf $p_{X\dot{X}\ddot{X}}(\cdot)$ through the relation [7]

$$p_{V\dot{V}\ddot{V}}(v,\dot{v},\ddot{v}) = \sum_{k=1}^m \frac{1}{|\mathbf{J}_3|} p_{X\dot{X}\ddot{X}}(x_k,\dot{x}_k,\ddot{x}_k) \tag{7}$$

where $\mathbf{J}_3$ is the Jacobian matrix given by

$$\mathbf{J}_3 = \begin{bmatrix} (\partial V/\partial X) & (\partial V/\partial \dot{X}) & (\partial V/\partial \ddot{X}) \\ (\partial \dot{V}/\partial X) & (\partial \dot{V}/\partial \dot{X}) & (\partial \dot{V}/\partial \ddot{X}) \\ (\partial \ddot{V}/\partial X) & (\partial \ddot{V}/\partial \dot{X}) & (\partial \ddot{V}/\partial \ddot{X}) \end{bmatrix} \tag{8}$$

the operator $|\cdot|$ denotes the absolute value of the determinant of a matrix, and m is the number of solution sets for $(x_k,\dot{x}_k,\ddot{x}_k)$ for the set of simultaneous equations (6), for given values of $V(t)=v$, $\dot{V}(t)=0$, and $\ddot{V}(t)=\ddot{v}$. It is obvious that m is the number of solutions for $x_k = g^{-1}[V(t)=v]$. The derivatives g' and g'', in Eq. (6), are evaluated at $X=x_k$. Thus, $\dot{x}_k = \{\dot{V}(t)=0\}/g'$ and is zero if $g' \neq 0$. The corresponding solution for $\ddot{x}_k = \{\ddot{V}(t)=\ddot{v}\}/g'$. It must be noted that in this formulation, a transformation is sought, which maps $(V,\dot{V},\ddot{V})$ into the $(X,\dot{X},\ddot{X})$-space and requires the solution of a set of three simultaneous equations defined in Eq. (6).

Instead, an alternative form for writing $p_{V\dot{V}\ddot{V}}(v,\dot{v},\ddot{v})$ is by mapping $(V,\dot{V})$ into the $(X,\dot{X})$-space. Thus, we write

$$p_{V\dot{V}\ddot{V}}(v,\dot{v},\ddot{v}) = \sum_{j=1}^r \frac{1}{|\mathbf{J}_2|} p_{X\dot{X}\ddot{V}}(x^{(j)},\dot{x}^{(j)},\ddot{v}) \tag{9}$$

where $\mathbf{J}_2$ is the Jacobian matrix given by

$$\mathbf{J}_2 = \begin{bmatrix} (\partial V/\partial X) & (\partial V/\partial \dot{X}) \\ (\partial \dot{V}/\partial X) & (\partial \dot{V}/\partial \dot{X}) \end{bmatrix} \tag{10}$$

and $(x^{(j)},\dot{x}^{(j)})$ are the solutions of the simultaneous equations $v = g(x)$ and $\dot{v} = g'\dot{x}$. Now, Eq. (9) can be further written as

$$p_{V\dot{V}\ddot{V}}(v,\dot{v},\ddot{v}) = \sum_{j=1}^r \frac{1}{|\mathbf{J}_2|} p_{\ddot{V}|X\dot{X}}(\ddot{v}) p_{X\dot{X}}(x^{(j)},\dot{x}^{(j)}) \tag{11}$$

Here, $p_{X\dot{X}}(x,\dot{x}) = p_X(x)p_{\dot{X}}(\dot{x})$ is the joint pdf of the Gaussian process $X(t)$, since $X(t) \perp \dot{X}(t)$.

Now, it can be seen from Eq. (6) that when conditioned on $(X,\dot{X})$, $\ddot{V}(t)$ is a linear sum of a constant and $\ddot{X}(t)$ and is hence Gaussian with parameters $\mu = E[\ \ddot{V}|_{X\dot{X}}]$ and $\sigma^2 = \mathrm{Var}[\ \ddot{V}|_{X\dot{X}}]$. Here, the operators $E[\cdot]$ and $\mathrm{Var}[\cdot]$ denote the mean and the variance, respectively. It can be seen that $\mathrm{Var}[\ \ddot{V}|_{X\dot{X}}] = (g'\sigma_{\ddot{X}})^2$ and since $|\mathbf{J}_3| = |(\partial \ddot{V}/\partial \ddot{X})\mathbf{J}_2| = |g'\mathbf{J}_2|$, Eq. (11) leads to identical results as Eq. (7). The usefulness of the second approach is manifested when $g(\cdot)$ is a function of vector Gaussian processes, and becomes clear in the formulation taken up in the following section.

2.2 Vector Case. We now consider the case when $V(t)$ is obtained as a nonlinear combination of a n-dimensional vector of mutually correlated, stationary Gaussian random processes, as given in Eq. (1). The first and second time derivatives of $V(t)$ are given by

$$\dot{V}(t) = \sum_{j=1}^n g_j'\dot{X}_j(t) \tag{12}$$

$$\ddot{V}(t) = \sum_{j=1}^{n}\sum_{k=1}^{n} g''_{jk}\dot{X}_j(t)\dot{X}_k(t) + \sum_{j=1}^{n} g'_j\ddot{X}_j(t) \tag{13}$$

Here, g'_j and g''_{jk} are, respectively, the first and second derivatives of $g[\cdot]$ with respect to the components of $\mathbf{X}$.

To proceed, we first introduce a set of transformations that had first been introduced in Ref. [5] in relation to the study of extremes of random processes of the type defined in Eq. (1). Using similar principles, we now rewrite

$$p_{V\dot{V}\ddot{V}}(v,0,\ddot{v}) = \int_{-\infty}^{\infty}\cdots\int_{-\infty}^{\infty} p_{X_2\cdots X_n\dot{X}_2\cdots\dot{X}_n V\dot{V}\ddot{V}}(x_2,\ldots,x_n,\dot{x}_2,\ldots,\dot{x}_n,v,0,\ddot{v})\mathrm{d}x_2\cdots\mathrm{d}x_n\mathrm{d}\dot{x}_2\cdots\mathrm{d}\dot{x}_n \tag{14}$$

Using the standard technique of transformation of random variables, we seek the relationship between the joint pdf's $p_{X_2\cdots X_n\dot{X}_2\cdots\dot{X}_n V\dot{V}\ddot{V}}(\cdot)$ and $p_{X_1\cdots X_n\dot{X}_1\cdots\dot{X}_n\ddot{V}}(\cdot)$. For a given time instant t, contributions to $p_{V\dot{V}\ddot{V}}(v,0,\ddot{v})$ can only come from points in $(X,\dot{X})$-space satisfying the two simultaneous equations, given by

$$g(X_1,X_2,\ldots,X_n) = v$$

$$\sum_{j=1}^{n} g'_j\dot{X}_j = \dot{v} \tag{15}$$

In principle, the simultaneous equations (15) can then be solved to give the only $(X_1,\dot{X}_1)$ points that contribute for given values of $(X_2=x_2,\ldots,X_n=x_n,\dot{X}_2=\dot{x}_2,\ldots,\dot{X}_n=\dot{x}_n)$, as well as for given values of $V=v$ and $\dot{V}=\dot{v}$. Assuming that for fixed values of $V=v$ and $\dot{V}=0$ there exists r solutions for $(X_1,\dot{X}_1)$ from Eq. (15), we rewrite Eq. (14) in the form

$$p_{V\dot{V}\ddot{V}}(v,0,\ddot{v}) = \sum_{j=1}^{r}\int\Omega_j\cdots\int\frac{1}{|\mathbf{J}_2|}p_{X_1\cdots X_n\dot{X}_1\cdots\dot{X}_n\ddot{V}}(x_1^{(j)},x_2,\ldots,x_n,\dot{x}_1^{(j)},\dot{x}_2,\ldots,\dot{x}_n,\ddot{v})\mathrm{d}x_2\cdots\mathrm{d}x_n\mathrm{d}\dot{x}_2\cdots\mathrm{d}\dot{x}_n \tag{16}$$

Here, Ω_j is the domain of integration determined by the permissible set of values $(x_2,\ldots,x_n,\dot{x}_2,\ldots,\dot{x}_n)$ for each solution for $(X_1,\dot{X}_1)$. $\mathbf{J}_2$ is the Jacobian matrix given by

$$\mathbf{J}_2 = \begin{bmatrix} (\partial V/\partial X_1) & (\partial V/\partial\dot{X}_1) \\ (\partial\dot{V}/\partial X_1) & (\partial\dot{V}/\partial\dot{X}_1) \end{bmatrix} \tag{17}$$

and the operator $|\cdot|$ denotes the absolute value of the determinant of the argument. Now, the joint pdf $p_{X_1\cdots X_n\dot{X}_1\cdots\dot{X}_n\ddot{V}}(\cdot)$ can be written as

$$p_{X_1\cdots X_n\dot{X}_1\cdots\dot{X}_n\ddot{V}}(x_1,\ldots,x_n,\dot{x}_1,\ldots,\dot{x}_n,\ddot{v}) = p_{\ddot{V}|\mathbf{X},\dot{\mathbf{X}}}(\ddot{v})p_{X_1\cdots X_n\dot{X}_1\cdots\dot{X}_n}(x_1,\ldots,x_n,\dot{x}_1,\ldots,\dot{x}_n) \tag{18}$$

Since $\mathbf{X}(t)$ is a vector of stationary Gaussian random processes, it follows that $\ddot{\mathbf{X}}(t)$ is jointly Gaussian. From Eq. (13), it is seen that $\ddot{\mathbf{V}}|_{\mathbf{X},\dot{\mathbf{X}}}$ is a linear sum of the components of $\ddot{\mathbf{X}}$ and is thus Gaussian with mean and variance, given by

$$\mu_{\ddot{V}|\mathbf{X},\dot{\mathbf{X}}} = E[\ddot{V}|\mathbf{X}=\mathbf{x},\dot{\mathbf{X}}=\dot{\mathbf{x}}] = \mathbf{G}\{E[\ddot{V}] + \mathrm{Cov}(\ddot{\mathbf{X}},\mathbf{Z})\mathrm{Cov}(\mathbf{Z},\mathbf{Z})^{-1}(\mathbf{z} - E[\mathbf{Z}])\}$$

$$\sigma^2_{\ddot{V}|\mathbf{X}\dot{\mathbf{X}}} = \mathrm{Var}[\ddot{V}|\mathbf{X}=\mathbf{x},\dot{\mathbf{X}}=\dot{\mathbf{x}}] = \mathbf{G}[\mathrm{Cov}(\ddot{\mathbf{X}},\ddot{\mathbf{X}}) - \mathrm{Cov}(\mathbf{Z},\ddot{\mathbf{X}})'\mathrm{Cov}(\mathbf{Z},\mathbf{Z})^{-1}\mathrm{Cov}(\mathbf{Z},\ddot{\mathbf{X}})]\mathbf{G}' \tag{19}$$

Here, $\mathbf{Z}=[\mathbf{X},\dot{\mathbf{X}}]$, $G_j=g_j$, and the operator $\mathrm{Cov}[\cdot]$ denotes the covariance. Since appropriate linear transformations can transform a vector of nonzero mean, mutually correlated Gaussian processes into a vector of zero-mean, mutually independent Gaussian processes [8], without loss of generality, it can be assumed that $\mathbf{X}$ constitutes a vector of zero-mean, mutually independent, stationary Gaussian processes. This leads to the following simplified forms for $\mu_{\ddot{V}|\mathbf{X}\dot{\mathbf{X}}}=\mu$ and $\sigma_{\ddot{V}|\mathbf{X}\dot{\mathbf{X}}}=\sigma$. It follows that Eq. (18) can be written in the form

$$p_{X_1\cdots X_n\dot{X}_1\cdots\dot{X}_n\ddot{V}}(\mathbf{x},\dot{\mathbf{x}},\ddot{v}) = \frac{1}{\sqrt{2\pi}\sigma}\exp\left[-\frac{(\ddot{v}-\mu)^2}{2\sigma^2}\right]\prod_{j=1}^{n}\{p_{X_j\dot{X}_j}(x_j,\dot{x}_j)\} \tag{20}$$

where $p_{X_j}(x_j)$ and $p_{\dot{X}_j}(\dot{x}_j)$ denote, respectively, the pdf's of X_j and $\dot{X}_j$. When appropriate transformations have been applied such that $\mathbf{X}$ constitutes a vector of zero-mean, mutually independent Gaussian random processes, we write

$$p_{X_j\dot{X}_j}(x_j,\dot{x}_j) = \frac{1}{2\pi\sigma_j\tilde{\sigma}_j}\exp\left[-\frac{x^2}{2\sigma_j^2} - \frac{\dot{x}^2}{2\tilde{\sigma}_j^2}\right] \tag{21}$$

where σ_j and $\tilde{\sigma}_j$ are, respectively, the standard deviations of X_j and $\dot{X}_j$. It must be noted that for stationary Gaussian processes, $X\perp\dot{X}$. Substituting Eq. (20) in Eq. (16), an expression for the joint pdf $p_{V\dot{V}\ddot{V}}(v,0,\ddot{v})$ is obtained.

The next step in determining the pdf for peaks of $V(t)$ lies in evaluating expressions in Eqs. (3)–(5). We first focus attention in evaluation of the integral of the type in Eq. (5). Substituting the expressions for the joint pdf for $p_{V\dot{V}\ddot{V}}(\cdot)$, we get

$$\begin{aligned}\mathcal{I}(v) &= \int_{-\infty}^{0}|\ddot{v}|p_{V\dot{V}\ddot{V}}(v,0,\ddot{v})\mathrm{d}\ddot{v} \\ &= \sum_{j=1}^{m}\left\{\int_{\Omega_j}\cdots\int\frac{p_{X_1\dot{X}_1}(x_1^j,\dot{x}_1^{(j)})}{|\mathbf{J}_2|}\times G_j(\mathbf{x},\dot{\mathbf{x}})\prod_{k=2}^{n}p_{X_k\dot{X}_k}(x_k,\dot{x}_k)\mathrm{d}x_2\cdots\mathrm{d}x_n\mathrm{d}\dot{x}_2\cdots\mathrm{d}\dot{x}_n\right\}\end{aligned} \tag{22}$$

where

$$\begin{aligned}G_j(\mathbf{x},\dot{\mathbf{x}}) &= \int_{-\infty}^{0}|\ddot{v}|p_{\ddot{V}|\mathbf{X},\dot{\mathbf{X}}}(\ddot{v}|\mathbf{X}=\mathbf{x},\dot{\mathbf{X}}=\dot{\mathbf{x}})\mathrm{d}\ddot{v} = \int_{-\infty}^{0}|\ddot{v}|\frac{1}{\sqrt{2\pi}\sigma}\exp\left[-\frac{(\ddot{v}-\mu)^2}{2\sigma^2}\right]\mathrm{d}\ddot{v} \\ &= -\frac{1}{2\sqrt{\pi}}\left[-\sqrt{2}\sigma\exp\left(-\frac{\mu^2}{2\sigma^2}\right) - \mu\sqrt{\pi}\,\mathrm{erf}\left\{\frac{\mu}{\sqrt{2}\sigma}\right\} + \mu\sqrt{\pi}\right]\end{aligned} \tag{23}$$

Here, the function $\mathrm{erf}\{x\}=(2\int_0^x\exp[-t^2]\mathrm{d}t)/\sqrt{\pi}$. The constant ψ in Eq. (4) can be evaluated, by integrating over v, as

$$\psi = \int_{-\infty}^{\infty}\int_{-\infty}^{0}|\ddot{v}|p_{V\dot{V}\ddot{V}}(v,0,\ddot{v})\mathrm{d}\ddot{v}\mathrm{d}v = \int_{-\infty}^{\infty}\mathcal{I}(v)\mathrm{d}v \tag{24}$$

The primary difficulties involved in evaluating $\mathcal{I}(v)$ in Eq. (22) are as follows:

- determining the domain of integration Ω_j, defined by the possible set of solutions for $(X_1^{(j)},\dot{X}_1^{(j)})$
- evaluation of the multidimensional integrals, which are of the form

$$\mathcal{I}_j = \int_{\Omega_j} \cdots \int f(x_1^{(j)}, x_2, \ldots, x_n, \dot{x}_1^{(j)}, \dot{x}_2, \ldots, \dot{x}_n) \prod_{k=2}^{n} p_{X_k \dot{X}_k} (x_k, \dot{x}_k) \mathrm{d}x_2 \cdots \mathrm{d}x_n \mathrm{d}\dot{x}_2 \cdots \mathrm{d}\dot{x}_n \tag{25}$$

where $f(\cdot) = |\mathbf{J}_2|^{-1} p_{X_1 \dot{X}_1}(x_1^j, \dot{x}_1^{(j)}) G_j(\mathbf{x}, \dot{\mathbf{x}})$. The dimension of the integrals in Eq. (25) is $2(n-1)$.

In this study, we adopt a numerical strategy to overcome these difficulties. This is discussed in the following section.

3 Numerical Algorithm

A crucial step in the above formulation lies in evaluating integrals of the type as in Eq. (25). Closed form solutions for $\mathcal{I}_j$ are possible only for a limited class of problems. Here, we propose the use of Monte Carlo methods, in conjunction with importance sampling to increase the efficiency, for evaluating these integrals. Equation (25) can be recast as

$$\mathcal{I}_j = \int_{-\infty}^{\infty} I[q(\mathbf{Z}) \leqslant 0] f(\mathbf{Z}) \frac{p_{\mathbf{Z}}(\mathbf{z})}{h_{\tilde{\mathbf{Z}}}(\mathbf{z})} h_{\tilde{\mathbf{Z}}}(\mathbf{z}) \mathrm{d}\mathbf{z} = \frac{1}{N} \sum_{j=1}^{N} I[q(\mathbf{Z}_j) \leqslant 0] f(\mathbf{Z}_j) \frac{p_{\mathbf{Z}}(\mathbf{z}_j)}{h_{\tilde{\mathbf{Z}}}(\mathbf{z}_j)} \tag{26}$$

where $\mathbf{Z} = [X_2, \ldots, X_n, \dot{X}_2, \ldots, \dot{X}_n]$, $h_{\tilde{\mathbf{Z}}}(\cdot)$ is the importance sampling pdf, and $I[\cdot]$ is an indicator function taking values of unity if $q(\mathbf{Z}) \leqslant 0$, indicating that the sample lies within the domain of integration Ω_j, and zero otherwise. Since the problem is formulated in the standard normal space $\mathbf{Z}$, $h_{\tilde{\mathbf{Z}}}(\cdot)$ can be taken to be Gaussian with unit standard deviation and shifted mean. The difficulty, however, lies in determining where should $h_{\tilde{\mathbf{Z}}}(\cdot)$ be centered. An inspection of Eq. (26) reveals that the form of the integrals is similar to reliability integrals, which are of the form

$$\mathcal{I}_j = \int_{-\infty}^{\infty} I[q(\mathbf{Z}) \leqslant 0] p_{\mathbf{Z}}(\mathbf{z}) \mathrm{d}\mathbf{z} \tag{27}$$

This implies that for efficient computation of the integrals, the importance sampling pdf $h_{\tilde{\mathbf{Z}}}(\cdot)$ may be centered around the design point [9,10] for the function $q(\mathbf{Z}) = 0$. If $q(\mathbf{Z})$ is available in explicit form, first order reliability methods [9,10] can be used to determine the design point. If $q(\mathbf{Z})$ is not available explicitly, an adaptive importance sampling strategy [11] can be adopted to determine the design point. In certain problems, the domain of integration, characterized by $q(\mathbf{Z}) = 0$, may consist of multiple design points or multiple regions, which contribute significantly to $\mathcal{I}_j$. This is especially true when $q(\mathbf{Z}) = 0$ is highly nonlinear, irregular, or consists of disjointed regions. In these situations, it is necessary to construct a number of importance sampling functions, with each function centered at various design points [12]. Techniques for determining multiple design points and regions of comparable importance have been discussed in the literature [12–15].

The steps for implementing the algorithm for numerical evaluation of integrals of the type in Eq. (25), have been developed in an earlier study by the present authors, with reference to development of extreme value distributions of non-Gaussian random processes [6]. However, for the sake of completeness, the sequential steps for implementing the algorithm are detailed below, with reference to the schematic diagram in Fig. 1.

1. Carry out pilot Monte Carlo simulations in the standard normal space. If there are too few samples in the failure domain, we carry out Monte Carlo simulations with a Gaussian importance sampling function with mean zero and a higher variance. On the other hand, if there are too few samples in the safe region, the variance of the importance sampling function is taken to be smaller. Repeat this step, till we have a reasonable number of samples in the failure and in the safe regions.
2. We sort the samples lying in the failure domain according to their distance from the origin.
3. A Gaussian importance sampling pdf is constructed, which is centered at the sample in the failure domain lying closest to the origin. Let this point be denoted by d_0 and its distance from the origin be denoted by β_0.
4. We check for samples in the failure domain, within a hypersphere of radius β_1, $\beta_1 - \beta_0 = \epsilon$, where ϵ is a positive number.
5. For samples lying within this hypersphere, we check for the sample d_1, which lies closest to the origin but is not located in the vicinity of d_0. This is checked by comparing the direction cosines of d_1 and d_0.
6. By comparing the direction cosines of all samples lying within the hypersphere of radius β_1, we can identify the number of design points. We construct importance sampling pdf's at each of these design points. If there exist no samples with direction cosines distinctly different from d_0, there is only one design point and a single importance sampling pdf is sufficient.
7. During importance sampling procedure corresponding to a design point, for each sample realization, we check if x_1 and $\dot{x}_1$ expressed in terms of the random variables $(Z_1, \ldots, Z_{2n-2})$ are real. The indicator function is assigned a value of unity if real, and zero otherwise.
8. An estimate of $\mathcal{I}_j$ is obtained from Eq. (26).

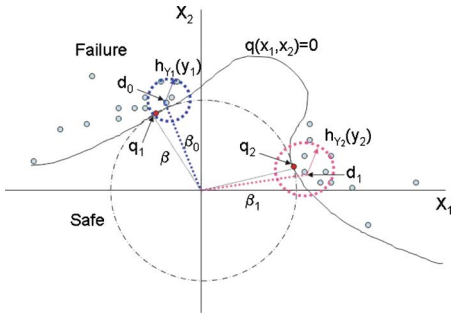

Fig. 1 Schematic diagram for numerical algorithm for evaluating multidimensional integrals: $q(x_1, x_2) = 0$ is the limit surface in the $X_1 - X_2$ random variable space, and $h_{Y_1}(y_1)$ and $h_{Y_2}(y_2)$ are two importance sampling pdf's; two design points at distance β from the origin

4 Expected Fatigue Damage

The approximate models for the peak density functions for the non-Gaussian loads can now be used to estimate the fatigue damage due to these loads. As is well known, fatigue damage occurs due to stress reversals and hence counting the number of cycles for a particular load constitutes an important aspect in fatigue analysis. The incremental fatigue damage due to a loading is proportional to the amplitude of a cyclic load and the total fatigue damage is estimated by assuming a suitable damage accumulation rule, such as the Palmgren–Miner's hypothesis [2]. Here, the fatigue damage at time t, denoted by $D(t)$, due to loading $V(t)$, is given by the relation

$$D(t) = \sum_{j=1}^{V(t)} \alpha s_j^{\beta} \tag{28}$$

where α and β are material properties, determined from experiments and s denotes the stress levels for the counted cycles. For random loads, the definition of a cycle, however, is not obvious. In these situations, the fatigue damage caused by a random load is

evaluated after estimating the number of cycles corresponding to various stress levels. Applying the Palmgren–Miner's rule, it can be shown that the expected fatigue damage per unit time, denoted by $E[d(t)]$, is given by the relation [16]

$$E[d(t)] = \nu_a \alpha \int_0^\infty s^\beta p_a(s) \mathrm{d}s \tag{29}$$

when the effect of mean stress is neglected. Here, $p_a(\cdot)$ is the pdf of the random amplitude levels, ν_a is the mean rate of occurrence for cycle denoted by (u,v), with $u \geqslant v$ such that u denotes a peak and v the corresponding valley in a completed cycle of a random stress history and the amplitude is defined as $s=(u-v)/2$.

As is well known, the estimate of the expected fatigue damage depends on the cycle counting method. Of the various cycle counting schemes available in the literature, the rain-flow counting scheme leads to estimates, which have the best agreement with those observed in experiments. However, the simplest approach is the peak-counting method, where a peak and a neighboring valley are assumed to constitute a cycle. This, in turn, requires the knowledge of the joint pdf $p_{uv}(\cdot)$. Also, since each cycle is associated with a peak, $\nu_a = \nu_p$, where ν_p is the mean rate of occurrence of peaks. Determining the joint pdf $p_{uv}(\cdot)$ even for this simple case is not straightforward and, only recently, some expressions have been developed for the special class of zero-mean, stationary Gaussian processes [17].

In this study, we consider a simpler model for the peak-counting method that has been used in the literature. Here, it is assumed that the damage is related to the peak distribution because its positive part agrees with the amplitude distribution. This leads to the following expression for $E[d(t)]$:

$$E[d(t)] = \tilde{\nu}_p \alpha \int_0^\infty s^\beta p_p(s) \mathrm{d}s \tag{30}$$

Since the peaks below zero are neglected, the expected number of cycles ν_a is lower than the expected number of peaks ν_p. To take this into account, we use $\tilde{\nu}_p$ in Eq. (30), which denotes the mean rate of occurrence of the positive peaks. We caution the reader that Eq. (30) gives an approximation for the true fatigue damage. We use Eq. (30) in this study, primarily to demonstrate the applicability of the developed peak distribution function for a non-Gaussian process. Examining the quality of this approximation is, however, beyond the scope of this paper.

We next need to estimate $\tilde{\nu}_p$. As a first step, we evaluate ν_p—the mean rate of occurrence of all peaks. This is equivalent to finding the mean rate of downcrossings of level zero by the process $\dot{V}(t)$ and is given by the celebrated Rice's formula [18]

$$\nu_p = -\int_{-\infty}^{0} \ddot{v} p_{\dot{V}\ddot{V}}(0,\ddot{v};t) \mathrm{d}\ddot{v} = -\int_{-\infty}^{\infty}\int_{-\infty}^{0} \ddot{v} p_{V\dot{V}\ddot{V}}(v,0,\ddot{v};t) \mathrm{d}\ddot{v}\mathrm{d}v \tag{31}$$

This is equivalent to Eq. (4) and has already been evaluated in Eq. (24). Using similar reasoning and since positive peaks imply $V(t) > v > 0$, the expression for $\tilde{\nu}_p$ can be obtained from

$$\tilde{\nu}_p = -\int_0^\infty \int_{-\infty}^{0} \ddot{v} p_{V\dot{V}\ddot{V}}(v,0,\ddot{v};t) \mathrm{d}\ddot{v}\mathrm{d}v = \int_0^\infty \mathcal{I}(v) \mathrm{d}v \tag{32}$$

Since the processes are assumed to be stationary, the expected fatigue damage due to a load process of time duration T is given by $E[D(T)] = TE[d(t)]$. In the following section, we illustrate the applicability of the proposed method through two numerical examples.

5 Numerical Examples and Discussions

The applicability of the proposed method is illustrated through two numerical examples. The first example, is a contrived numerical example where we assume that the function $g(\cdot)$ in Eq. (1) is linear. We use this example to focus on the numerical aspects of the proposed method. In the second example, we compute the peak distribution for the developed Von Mises stress at a specified location of a seismically loaded nuclear power plant.

5.1 Example 1: Peak Distribution for a Gaussian Process. We consider the compound process

$$V(t) = \sum_{j=1}^{3} X_j(t) = g[X_1(t), X_2(t), X_3(t)] \tag{33}$$

where $\{X_j(t)\}_{j=1}^3$ are assumed to be zero-mean, mutually independent, stationary Gaussian processes, with specified power spectral density (PSD) functions given by

$$S_{jj}(\omega) = \frac{S_j^2}{\sqrt{\pi \alpha_j}} \frac{1}{(2\eta_j \Omega_j)^2 + (\omega^2 - \Omega_j)^2} \exp\left[-\frac{\omega^2}{\beta \gamma_j}\right], \quad j = 1,2,3 \tag{34}$$

Here, we assume that $S_j = j\sqrt{2}$, $\gamma_j = 100j$, $\Omega_1 = 4\pi$, $\Omega_2 = 10\pi$, $\Omega_3 = 20\pi$, and $\beta = 4$. Since $V(t)$ is a linear combination of $\{X_j(t)\}_{j=1}^3$, it is a zero-mean, stationary Gaussian random process with PSD $S_{VV}(\omega) = \Sigma_{j=1}^3 S_{jj}(\omega)$. A closed form analytical expression for the pdf of the peaks (p) for $V(t)$ is available [3] and is given by

$$p_p(u) = \frac{\sqrt{1-\alpha_2^2}}{\sqrt{2\pi}\sigma} \exp\left[-\frac{(u-\mu)^2}{2(1-\alpha_2^2)\sigma^2}\right] + \frac{\alpha_2 (u-\mu)}{2\sigma^2} \exp\left[-\frac{(u-\mu)^2}{2\sigma^2}\right]\left\{1 + \mathrm{erf}\left[\frac{\alpha_2 (u-\mu)}{\sigma\sqrt{2(1-\alpha_2^2)}}\right]\right\} \tag{35}$$

where μ and σ are the mean and standard deviations of $V(t)$, $\alpha_2 = \lambda_2 / \sqrt{\lambda_0 \lambda_4}$ is a bandwidth parameter defined in the range zero to unity, and λ_j are the spectral moments given by

$$\lambda_j = 2\int_0^\infty \omega^j S_{VV}(\omega) \mathrm{d}\omega, \quad j = 0, \ldots, 4 \tag{36}$$

We compare the predictions made by the proposed method with the exact solution given by Eq. (35), in Fig. 2. We observe that the predictions by the proposed method compare quite well with those obtained from Eq. (35). However, when the function $g(\cdot)$ is nonlinear, it is not always possible to obtain a closed form expression for the peak density function. In such cases, the predictions made by full scale Monte Carlo simulations serve as the benchmark. In the Monte Carlo method, we digitally simulate an ensemble of time histories for the component processes $\{X_j(t)\}_{j=1}^3$ and compute $V(t)$ from Eq. (1), using the spectral decomposition method [21,22]. Next, we use the WAFO toolbox [23], to extract the peaks corresponding to each sample time history of $V(t)$. Subsequently, by statistical processing of the extracted peaks, we construct the peak density function for $V(t)$. The peak density function constructed in this manner is subject to statistical fluctuations. However, as the ensemble size (N) is increased, the statistical fluctuations die down leading to stable estimates for the peak density function. This is illustrated in Fig. 2. We see that the pdf constructed using $N=20$ and $N=200$ is subject to large fluctuations, though the fluctuations for $N=200$ are relatively smaller. Increasing the ensemble size further tenfold, we observe that the pdf with $N=2000$ leads to a fairly smooth pdf and compares very well with the exact pdf. This lends credence to the belief that the Monte Carlo method can serve as a benchmark to compare the predictions obtained by the proposed method, in situations where a closed form expression for the peak pdf is not available.

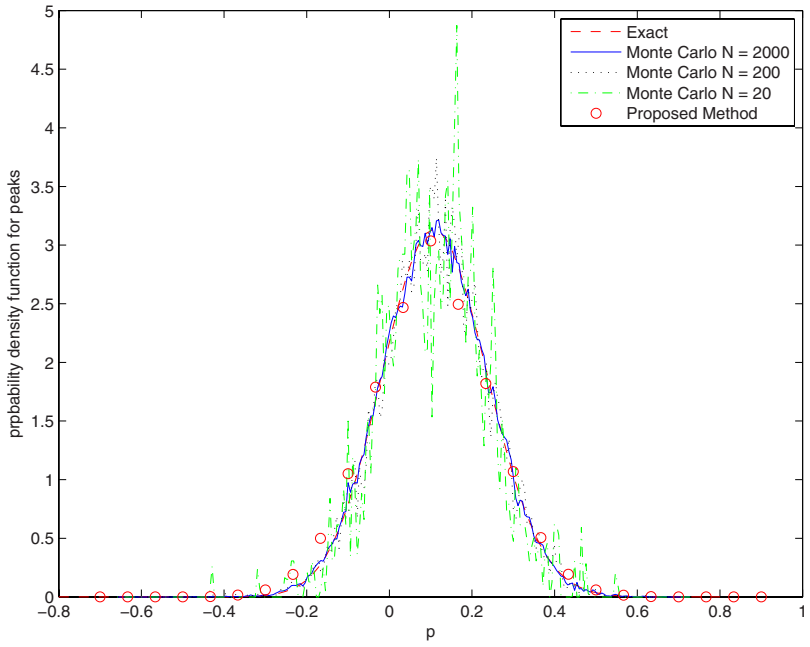

Fig. 2 Probability density functions for peaks for $V(t)$, example 1

While it is difficult to *a priori* determine the ensemble size N such that the estimates obtained are stable, a reasonable criterion for determining N could be given by

$$\sum_{i=1}^{M} [p_{N_j}(u_i) - p_{N_{j-1}}(u_i)]^2 \leqslant \epsilon \tag{37}$$

where M denotes the number of discretized segments of the argument (the x-axis) for the peak pdf, $p_{N_j}(u_i)$ denotes the abscissa for the peak pdf corresponding to the ith argument, obtained with a sample size of N_j, and ϵ is a tolerance limit. It is obvious that $\Sigma_{i=1}^{M}[p_{N_j}(u_i) - p_{N_{j-1}}(u_i)]^2$ asymptotically approaches zero as N increases. It must be noted that simulation of N samples of a time history of duration T seconds is equivalent to simulating a single time history of duration NT seconds and the associated computational problems are identical in both cases.

Since in the next example, we benchmark the predictions of the proposed method with full scale Monte Carlo simulations, it is appropriate to consider the sources of error in the proposed method also. It must be emphasized here that the expression for the joint pdf $p_{V\dot{V}\ddot{V}}(v,0,\ddot{v})$ in Eq. (20) is exact assuming that Eq. (15) can be solved exactly. Then, the approximation in evaluating $p_p(u)$ (see Eq. (5)) lies in the evaluation of the numerator (Eq. (22)) and the denominator (Eq. (24)). In this paper, we employ the Monte Carlo method to estimate the multidimensional integral in Eq. (22) and the convergence rate of the associated errors is of the $O(N^{1/2})$. However, in situations where exact solutions for Eq. (15) are neither available nor straightforward, appropriate numerical algorithms need to be employed to determine the solutions. These numerical solutions have errors, which are dependent on the error tolerances used in the algorithms. Moreover, in situations where there exist multiple solutions, depending on the nonlinearity involved and the tolerance levels of the algorithms, there is a possibility that some solutions could be missed. However, in most practical problems, it is usually easy to determine the number of possible solutions and search accordingly. A further source of error in evaluating $\mathcal{I}(v)$ lies in numerically determining the domain of integration Ω_j in Eq. (22). Application of FORM in identifying the design points for centering the importance sampling pdf's introduces further numerical errors. However, if the sample size N is sufficiently large, most of these errors turn out to be quite small. In this study, we have considered $N=1\times10^6$. While computing the denominator from Eq. (24), there are three sources of errors: (a) since the integrand is the estimate of the multidimensional integration of Eq. (22), the associated error gets carried over, (b) error associated with the numerical scheme used in the integration, and (c) the cut-off points considered for the integration range and the number of discrete points considered within the interval while evaluating the integral. In this paper, we have chosen the cut-off points (v_i), such that, $\mathcal{I}(v_i)/\mathcal{I}_{\max}(v) \leqslant \delta$, where v lies within the range defined by the cut-off points, $\mathcal{I}_{\max}(v)$ is the maximum value of $\mathcal{I}(\cdot)$ evaluated within the range, and δ is a prescribed tolerance limit of $O(10^{-4})$.

The parameters $\{\eta_j\}_{j=1}^{3}$ in Eq. (34) are varied so that one can observe the performance of the proposed method as a function of the spectral bandwidth of the process $V(t)$. The bandwidth of the process $V(t)$ is measured according to the definition in Ref. [25] and is given by

$$q = \sqrt{1 - \frac{\lambda_1^2}{\lambda_0 \lambda_2}} \tag{38}$$

Figure 3 illustrates the peak pdf for two cases, $q=0.4771$ and $q=0.3333$. It can be observed that the proposed method leads to fairly good match with the exact. This seems to indicate that at least for Gaussian processes, the spectral shape of the process does not have much of a bearing with the accuracy of the proposed method.

The CPU time required by the proposed method is 23.31 s. In contrast, the CPU times consumed in the Monte Carlo simulations are 11.83 s, 118.70 s, and 1458.5 s when the sample sizes are, respectively, 20, 200, and 2000. Thus, in this example, the proposed method requires approximately 2% of the CPU time required for full scale Monte Carlo simulations. The computational effort required in the proposed method is significantly less in comparison with the full scale Monte Carlo simulations for two reasons: (a) The proposed method requires digital simulation of a vector of standard normal random variables, which is straightforward and requires much less memory space than simulating a vector of random processes. (b) Using the proposed method, the

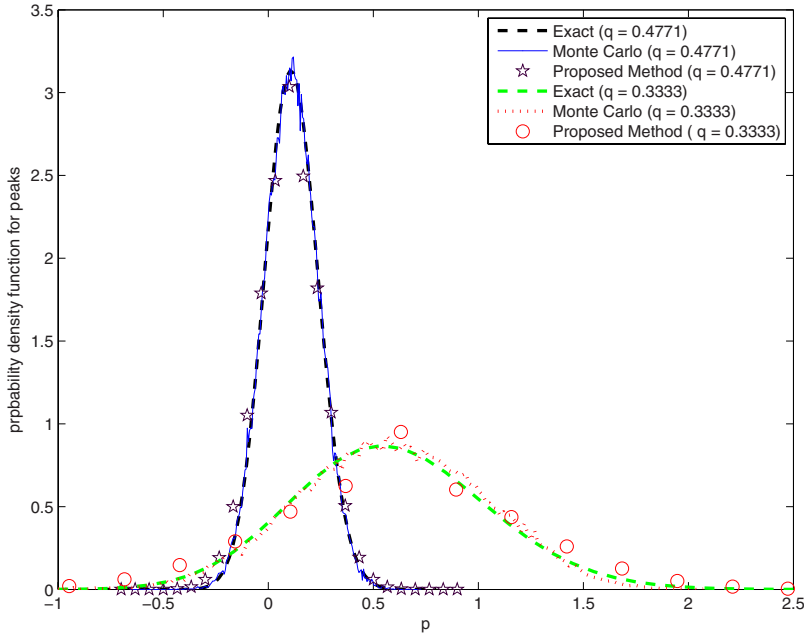

Fig. 3 Effect of shape factor of $S_{VV}(\omega)$ on pdf for peaks for $V(t)$, example 1

peak pdf needs to be evaluated at a few points and the full pdf may be obtained by interpolation. On the other hand, in the full scale Monte Carlo method, the ensemble size N has to be sufficiently large for the statistical fluctuations to die down before one can have stable estimates of the peak pdf.

5.2 Example 2: Peak Distribution for Von Mises Stress in a Seismically Excited Structure. We seek the expected fatigue damage due to the Von Mises stress, $V(t)$, developed at the base of a support for a fire-water pipeline, in a seismically excited nuclear power plant. The earthquake ground accelerations, specified at the reactor base level, are modeled as a vector of stationary Gaussian random processes and are characterized through the PSD matrix, defined along the principal components of the seismic excitations. The principal components are assumed to be inclined at a specified angle in the horizontal plane with respect to the coordinate system, in which the reactor structure is modeled. Thus, an appropriate transformation leads to the fully populated PSD matrix for the seismic accelerations at the reactor base. In the analysis procedure adopted, the reactor building, the piping structure at a specified level, and the supporting structure considered in the fatigue analysis are, respectively, assumed to be the primary, secondary, and tertiary structures. Finite element (FE) method has been used to model these structures; see Ref. [19] for details on these FE models and the analysis procedure. A random vibration analysis is carried out to determine the auto- and cross-PSD functions for the absolute ground accelerations at the piping floor level. Here, all the three components turn out to be mutually correlated. The piping structure considered has 21 similar supporting structures. A schematic diagram of one of these supports is shown in Fig. 4. In the FE model used for the piping structure, the supports are represented as a set of discrete linear springs. The PSDs of the transverse forces imparted on the supports by the pipes due to earthquake loading are computed using random vibration analysis on the piping structure FE model. These PSDs are used as inputs in the random vibration analysis of the supports. The details of these calculations are available in Refs. [19,20]. In this example, we consider the fatigue damage in one such support.

The support, built up of two channel sections (see Fig. 4), is modeled as a cantilever beam. $Q_1(t)$ and $Q_2(t)$ are reaction forces transmitted from the piping structure to the pipe support structure. The analysis has been carried out by assuming a plane-stress model for the support structure. Thus, the stress vector is assumed to consist of three nonzero components $\{Y_i(t)\}_{i=1}^3$. Since the excitations have been assumed to be zero-mean Gaussian processes and structure behavior is assumed to be linear, the stress components $\{Y_i(t)\}$ constitute a vector of zero-mean, mutually correlated, Gaussian random processes. The auto- and cross-PSD functions of these stress components, $S_{ij}(\omega)$, $(i,j=1,2,3)$, are obtained from a random vibration analysis. Figure 5 illustrates the auto-PSD functions of the stress components $\{Y_i(t)\}_{i=1}^3$ and the magnitudes of their cross-PSDs. The bandwidths of the processes $\{Y_i(t)\}_{i=1}^3$, measured in terms of the spectral parameter q in Eq. (38), are, respectively, 0.4796, 0.4762, and 0.4315. This indicates that the processes $\{Y_i(t)\}_{i=1}^3$ lie in between the spectrum of strictly narrow-band and strictly broad-band (white noise) processes.

The Von Mises stress, $V(t)$, is related to the stress components $\{Y_i(t)\}_{i=1}^3$ through the relation

$$V(t) = \{Y_1^2(t) + Y_2^2(t) + 3Y_3^2(t) - Y_1(t)Y_2(t)\}^{0.5} \tag{39}$$

Thus, $V(t)$ is a stationary non-Gaussian random process whose pdf is not known. The time derivative and the double time derivative of $V(t)$ are given by

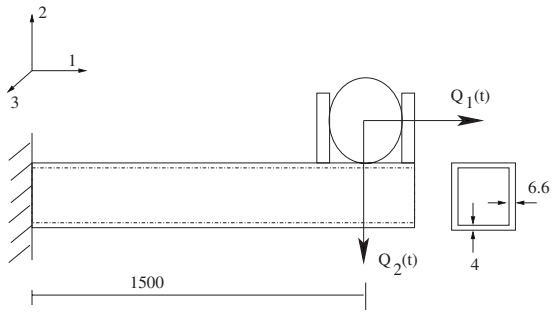

Fig. 4 Schematic diagram of the support for the fire-water system in a nuclear power plant, all dimensions are in mm; example 2

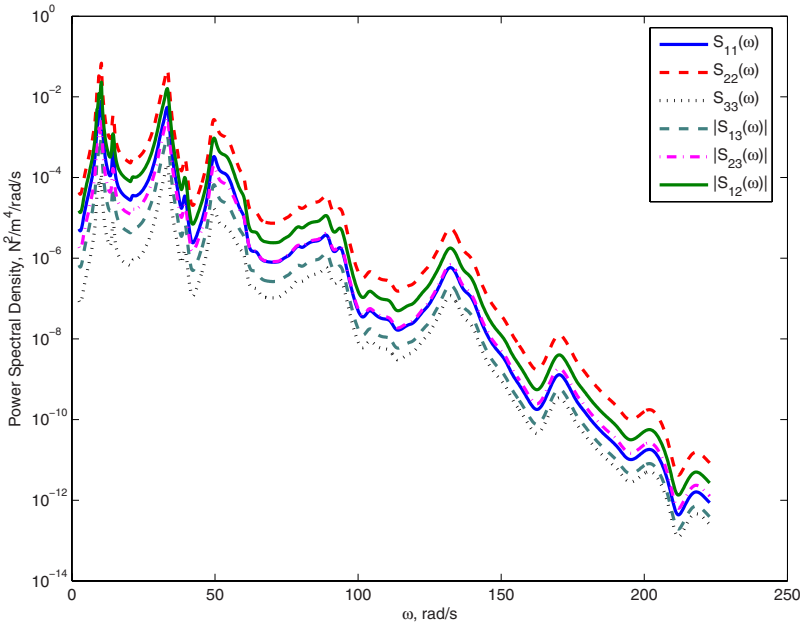

Fig. 5 Power spectral density functions for the stress components at the root of the cantilever, example 2

$$\dot{V}(t) = \frac{1}{2V}\{2Y_1\dot{Y}_1 + 2Y_2\dot{Y}_2 + 6Y_3\dot{Y}_3 - \dot{Y}_1Y_2 - Y_1\dot{Y}_2\} \tag{40}$$

$$\ddot{V} = -\frac{\dot{V}^2}{V} + \frac{1}{2V}\{2\dot{Y}_1^2 + 2Y_1\ddot{Y}_1 + 2\dot{Y}_2^2 + 2Y_2\ddot{Y}_2 + 6\dot{Y}_3^2 + 6Y_3\ddot{Y}_3 - \ddot{Y}_1Y_2 - 2\dot{Y}_1\dot{Y}_2 - Y_1\ddot{Y}_2\} \tag{41}$$

At any instant of time, $\mathbf{Y}=[Y_1, Y_2, Y_3]$ constitute a vector of mutually correlated random variables with covariance matrix $\mathbf{C_Y} = \mathbf{LL}'$. Here, the superscript, $'$, denotes matrix transpose operator and $\mathbf{L}$ is the lower triangular matrix obtained by Cholesky decomposition of $\mathbf{C_Y}$. Using the transformation $\mathbf{Y}=\mathbf{LX}$ enables expressing V, at any time instant t, in terms of a vector of mutually independent Gaussian random variables $\mathbf{X}=[X_1, X_2, X_3]$. Assuming that at a time instant t, $X_2=x_2$, $X_3=x_3$, $\dot{X}_2=\dot{x}_2$, $\dot{X}_3=\dot{x}_3$, $V=v$, and $\dot{V}=0$, solutions for X_1 are obtained from the solution of the equation

$$\alpha X_1^2 + \beta X_1 + \gamma = 0 \tag{42}$$

where

$$\alpha = L_{11}^2 + 3L_{31}^2 + L_{21}^2 - L_{11}L_{21}$$

$$\beta = (2L_{22}L_{21} - L_{11}L_{22})x_2 + 6L_{31}(L_{32}x_2 + L_{33}x_3)$$

$$\gamma = 3(L_{32}x_2 + L_{33}X_3)^2 + L_{22}^2x_2^2 - v^2 \tag{43}$$

Here, the subscripts i and j in L_{ij} denote, respectively, the ith row and jth column of matrix $\mathbf{L}$. It is evident from Eq. (42) that real solutions are obtained when $\beta^2 - 4\alpha\gamma \geq 0$. This condition also defines the domain of integration, which leads to admissible solutions for X_1. Equation (42) being quadratic in X_1, there exist two solutions for $X_1 = (-\beta \pm \sqrt{\beta^2 - 4\alpha\gamma})/(2\alpha)$. The corresponding pair of solutions for $\dot{X}_1 = -\psi_n/\psi_d$, where

$$\psi_n = 2L_{44}y_1 + 2L_{54}y_2 + 6L_{64}y_3 - L_{44}y_2 - L_{54}y_1$$

$$\psi_d = 2y_1(L_{41}x_1 + L_{42}x_2 + L_{43}x_3) + 2y_2(L_{51}x_1 + L_{52}x_2 + L_{53}x_3 + L_{55}\dot{x}_2) + 6y_3(L_{61}x_1 + L_{62}x_2 + L_{63}x_3 + L_{65}\dot{x}_2 + L_{66}\dot{x}_3) - y_2(L_{41}x_1 + L_{42}x_2 + L_{43}x_3) - y_1(L_{51}x_1 + L_{52}x_2 + L_{53}x_3 + L_{55}\dot{x}_2) \tag{44}$$

The mean and the variance for the conditioned random variable $V|_{\mathbf{Y}\dot{\mathbf{Y}}}$ are computed from Eq. (19), where

$$\mu = (2\dot{y}_1^2 + 2\dot{y}_2^2 + 6\dot{y}_3^2 - 2\dot{y}_1\dot{y}_2)/(2v)$$

$$\sigma^2 = \sum_{j=1}^{3}\sum_{k=1}^{3} b_j b_k E[\ddot{Y}_j\ddot{Y}_k] \tag{45}$$

where $b_1=(2y_1-y_2)/(2v)$, $b_2=(2y_2-y_1)/(2v)$, and $b_3=6y_3/(2v)$. The expectations, $E[\ddot{Y}_i\ddot{Y}_j]$, are obtained from the auto- and cross-PSD of the components of $\{Y_j\}_{j=1}^3$, and are expressed as

$$E[\ddot{Y}_i\ddot{Y}_j] = \Re\left\{\int_{-\infty}^{\infty} \omega^4 S_{ij}(\omega)\mathrm{d}\omega\right\} \tag{46}$$

Here, the operator $\Re\{\cdot\}$ denotes the real part when $i \neq j$ and is superfluous when $i=j$.

The integrals $\mathcal{I}_j$ that need to be solved are now four-dimensional and the domain of integration Ω_j is defined by the region in the four dimensional space spanned by the vector $[X_2, X_3, \dot{X}_2, \dot{X}_3]$, such that $\beta^2 - 4\alpha\gamma \geq 0$. We now implement the numerical algorithm, discussed in sec. 3, to evaluate the integrals. We observe that each Ω_j is characterized by two design points. In constructing the Gaussian importance sampling pdf for X_2 and X_3, we assume that the mean to be situated at this design point is obtained from the algorithm. The variance is taken to be such that the coefficient of variation is equal to 0.60. From the formulation, it can be seen that no computational efficiency is achieved by constructing importance sampling pdfs for $\dot{X}_2$ and $\dot{X}_3$. Thus, the importance sampling pdf is two-dimensional only. We construct a vector of mutually independent, Gaussian random variables consisting of 1×10^6 samples and estimates of the integrals $\mathcal{I}(v)$ are

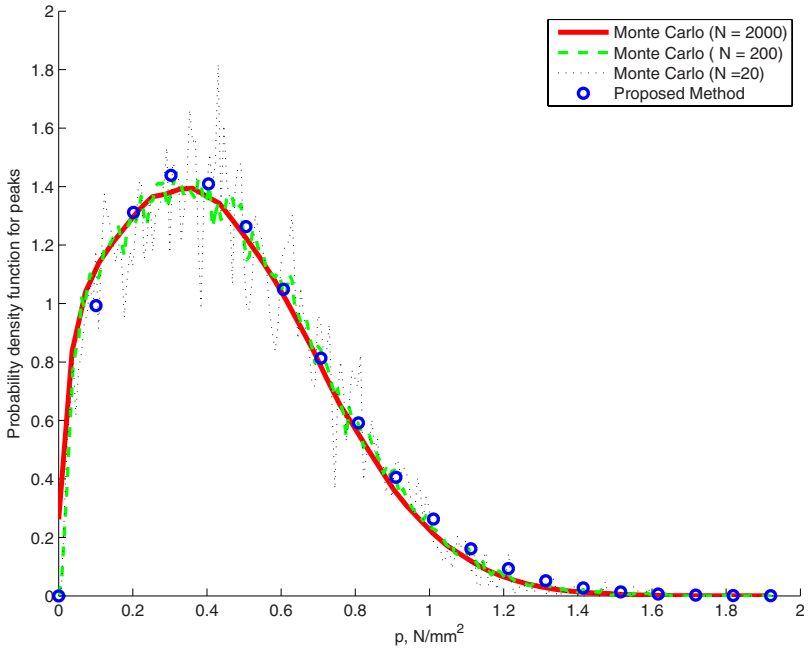

Fig. 6 Probability density functions for the peaks of Von Mises stress, example 2

obtained by computing the mean, from Eq. (26), for various values of v. The constant ψ, in Eq. (24), is subsequently computed numerically by applying the trapezoidal rule of integration. The pdf and the corresponding PDF, for the peaks for $V(t)$, estimated using the proposed method, are, respectively, shown in Figs. 6 and 7. These results are compared with the pdf and PDF of the peaks for $V(t)$ obtained from full scale Monte Carlo simulations on an ensemble of size 2000 samples. In the Monte Carlo method, from the knowledge of the PSD matrix of $\{Y_j(t)\}_{j=1}^3$, we construct an ensemble of vector of mutually correlated processes $\{Y_j(t)\}_{j=1}^3$ using the well-known spectral decomposition method [21,22]. Subsequently, samples of $V(t)$ are obtained by applying the transformation in Eq. (39). Using the WAFO toolbox [23], we estimate the peaks corresponding to each sample time history of $V(t)$. Subsequently, statistical processing of the peaks, we construct the pdf and the corresponding PDF. These serve as the benchmark, with which we compare the predictions made by the proposed method. As can be seen from Figs. 6 and 7, the predictions compare favorably with those obtained from Monte Carlo simulations. The slight overestimation of the peak pdf using the proposed method

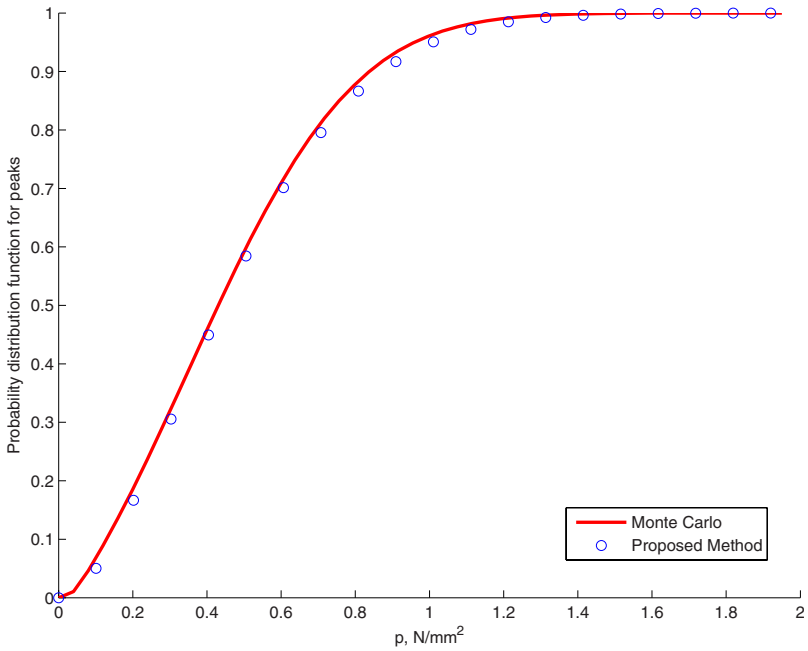

Fig. 7 Probability density functions for the peaks of Von Mises stress, example 2

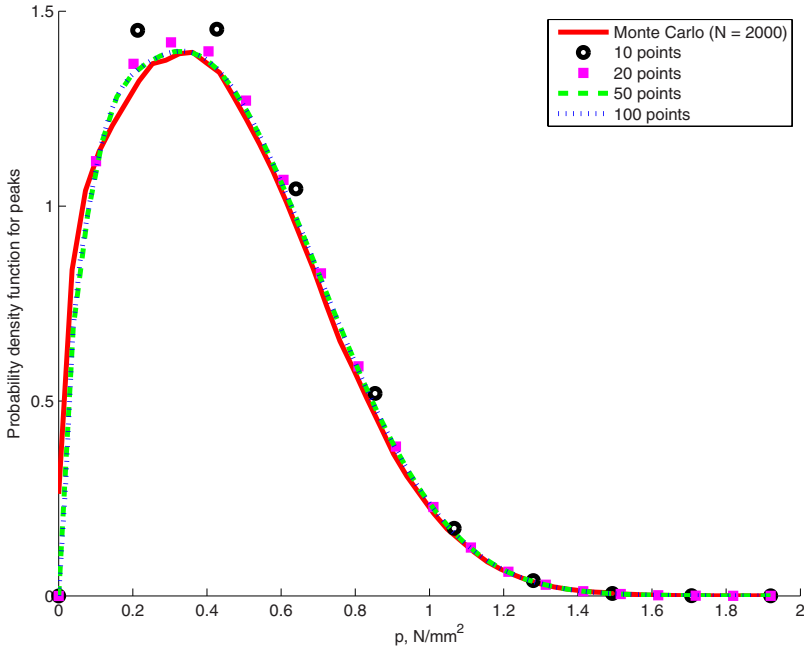

Fig. 8 Effect of discretization on the overall accuracy of the estimated pdf of the peaks of Von Mises stress, example 2

can be attributed to the numerical errors in computing ψ when a coarse grid is used for the numerical integration in Eq. (24). This error can be minimized by considering a finer grid size; see Fig. 8 where a comparison of the predicted peak pdf is illustrated when the pdf is evaluated at 10, 20, 50, and 100 points, respectively. However, in most practical situations, the error involved is too small to be of much significance, especially in view of the increased computational cost.

We also investigate the statistical stability of the solution obtained from Eq. (26) and its dependence on the sample size of the vector of random variables and the coefficient of variation (cov) of the importance sampling pdf. Figures 9 and 10 compare the predicted peak pdfs using the proposed method for different values of Cov when the sample sizes are, respectively, 1×10^4 and 1×10^6. We observe that the predictions are sensitive to changes in Cov values when 1×10^4 samples are used. This can be attributed to the fact that the importance sampling variance influences the number of samples lying within the integration domain and a smaller sample size leads to statistical fluctuations. These fluctua-

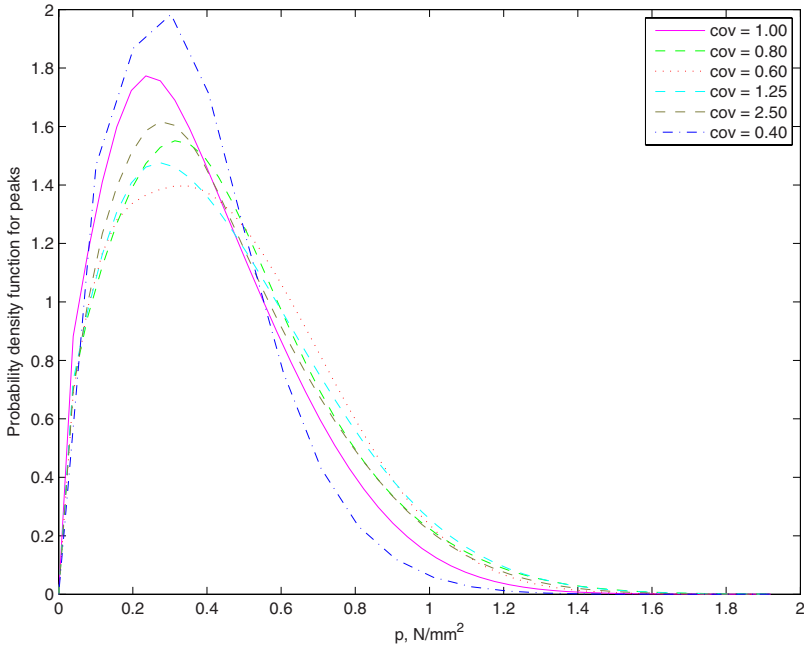

Fig. 9 Probability density functions for peaks of Von Mises stress, estimated using the proposed method, with sample size 1×10^4, example 2

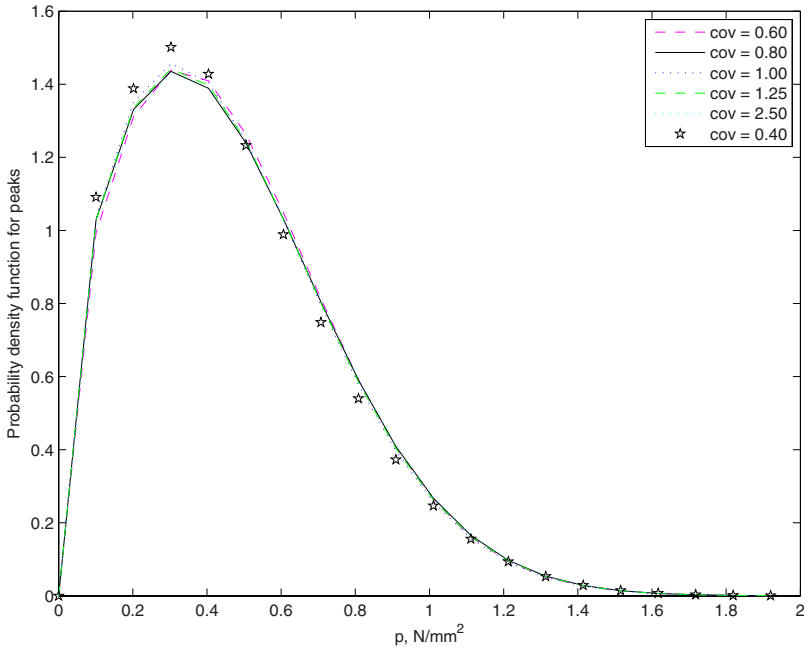

Fig. 10 Probability density functions for peaks of Von Mises stress, estimated using the proposed method, with sample size 1×10^6, example 2

tions die down when the sample size is increased and this is illustrated in Fig. 10, where it is observed that the sensitivity of the importance sampling pdf is much less. Therefore, a criterion for ascertaining whether the sample size is large enough could be by checking the sensitivity of the solution for the integral in Eq. (26) for different values of Cov for the importance sampling pdf. If changing the Cov has a little effect on the estimate, one can accept the sample size to be sufficiently large. This check may be applied at a single point only.

In Fig. 6, we also present the estimated pdf obtained when the sample sizes in the full scale Monte Carlo simulations are $N=200$ and $N=20$. The CPU time required using the proposed method is 106.95 s when the peak pdf is evaluated at 10 points and is 198.74 s when evaluated at 20 points. The required CPU times for Monte Carlo simulations are 34.02 s, 341.13 s, and 3737.30 s when the sample sizes are, respectively, 20, 200, and 2000. From Fig. 6, we observe that the accuracy obtained by Monte Carlo simulations when $N=200$ is quite acceptable. This implies that the savings in CPU time using the proposed method is about 70–40%.

For the sake of illustration, we consider hypothetical values for the fatigue constants in Eq. (30) and assume that $\alpha=1\times10^{-2}$ and $\beta=2$. The resultant expected fatigue damage, for a loading of time duration $T=20$ s, is found to be 0.0225. Note that $V(t)$ being a strictly positive random process, all peaks are positive and hence $\nu_p=\tilde{\nu}_p$. The corresponding expected fatigue damage obtained from Monte Carlo simulations, when the peak-counting method as given in Eq. (30) is employed, turns out to be 0.0294.

6 Concluding Remarks

A methodology has been developed for approximating the pdf and PDF for the peaks of a special class of non-Gaussian loads, obtained as nonlinear combination of a vector of mutually correlated, stationary Gaussian random processes. This, in turn, required developing models for the joint pdf for the non-Gaussian process, and its first and second time derivatives. The developed models for the peak pdf for the non-Gaussian processes have subsequently been shown to be useful in estimating the expected fatigue damage when the peak-counting method is employed to estimate the equivalent number of cycles in the random load.

A key feature in the development of the proposed method lies in the assumption that for high thresholds, the number of level crossings of a non-Gaussian process can be modeled as a Poisson point process. The assumption of the outcrossings being Poisson distributed has been proved to be mathematically valid for Gaussian processes when the thresholds asymptotically approach infinity [24]. However, it has been pointed out that for threshold levels of practical interest, this assumption results in errors whose size and effect depend on the bandwidth of the processes [25]. While it can be heuristically argued that for high thresholds, the outcrossings of non-Gaussian processes can be viewed to be statistically independent and hence can indeed be modeled as a Poisson point process, to the best of the authors' knowledge, studies on the validity of this assumption do not exist in the literature. The approximations developed in this paper are thus expected to inherit the associated inaccuracies and limitations, due to this assumption.

It is well known that the peak-counting method provides a conservative estimate of the expected fatigue damage. Studies on the more accurate rain-flow fatigue damage due to non-Gaussian loads obtained as nonmonotonic transformations of a scalar Gaussian load and a nonlinear combination of vector Gaussian loads have been recently carried out [26,27]. Nevertheless, the proposed method provides a fast and computationally cheap estimate for the expected fatigue damage. These results can subsequently be used to predict the lifetime of aging structures.

It must be emphasized here that the savings in CPU time using the proposed method when compared with Monte Carlo simulations would depend on the complexity of the problem, the type of nonlinear function in Eq. (1), and the difficulty involved in numerically establishing the domain of integration in Eq. (25). In fact, for certain problems, it might be quite infeasible to use the proposed method, especially if the solution of the nonlinear equations in Eq. (15) becomes too complex. Thus, while the Monte Carlo simulation technique provides the only solution method for many complicated problems, for certain limited class of problems,

the proposed method provides an alternative (and perhaps less computationally demanding) technique. The proposed method needs to be viewed accordingly.

References

[1] Nigam, N. C., 1983, *Introduction to Random Vibrations*, MIT, MA.
[2] Sobczyk, K., and Spencer, B. F., 1992, *Random Fatigue: From Data to Theory*, Academic, San Diego, CA.
[3] Lutes, L. D., and Sarkani, S., 2004, *Random Vibrations: Analysis of Structural and Mechanical Systems*, Elsevier Butterworth-Heinemann, Burlington, MA.
[4] Solnes, J., 1997, *Stochastic Processes and Random Vibrations*, Wiley, New York.
[5] Naess, A., 1985, "Prediction of Extremes of Stochastic Processes in Engineering Applications With Particular Emphasis on Analytical Methods," Ph.D. thesis, Norwegian Institute of Technology, Trondheim.
[6] Gupta, S., and van Gelder, P., 2006, "Extreme Value Distributions for Nonlinear Transformations of Vector Gaussian Processes," Probab. Eng. Mech., **22**, pp. 136–149.
[7] Papoulis, A., 1997, *Probability, Random Variables and Stochastic Processes*, McGraw-Hill, New York.
[8] Ang, A. H. S., and Tang, W. H., 1984, *Probability Concepts in Engineering Planning and Design. Volume II: Decision, Risk and Reliability*, Wiley, New York.
[9] Ditlevsen, O., and Madsen, H. O., 1996, *Structural Reliability Methods*, Wiley, Chichester.
[10] Melchers, R. E., 1999, *Structural Reliability Analysis and Prediction*, Wiley, Chichester.
[11] Bucher, C. G., 1988, "Adaptive Importance Sampling—An Iterative Fast Monte Carlo Procedure," Struct. Safety, **5**, pp. 119–126.
[12] Karamchandani, A., Bjerager, P., and Cornell, C. A., 1989, "Adaptive Importance Sampling," *Proceedings of the Fifth International Conference on Structural Safety and Reliability*, A. H. S. Ang, and M. Shinozuka, and G. I. Schueller, eds., New York, pp. 855–862.
[13] Breitung, K., and Faravelli, L., 1996, "Response Surface Methods and Asymptotic Approximations," *Mathematical Models for Structural Reliability Analysis*, F. Casciati, and J. B. Roberts, eds. CRC, Boca Raton, FL, Chap. 5.
[14] Der Kiureghian, A., and Dakessian, T., 1998, "Multiple Design Points in First and Second Order Reliability," Struct. Safety, **20**, pp. 37–49.
[15] Gupta, S., and Manohar, C. S., 2004, "An Improved Response Surface Method for the Determination of Failure Probability and Importance Measures," Struct. Safety, **26**, pp. 123–139.
[16] Tovo, R., 2002, "Cycle Distribution and Fatigue Damage Under Broad-Band Random Loading," Int. J. Fatigue, **24**, pp. 1137–1147..
[17] Lutes, L. D., 2006, "Joint Distribution of Peaks and Valleys in a Stochastic Process," *Proceedings of the Fifth Computational Stochastics Mechanics Conference*, Rhodos, Greece.
[18] Rice, S. O., 1954, "A Mathematical Analysis of Noise," *Selected Papers in Random Noise and Stochastic Processes*, ed., Dover Publications New York, pp. 133–294.
[19] Gupta, S., and Manohar, C. S., 2006, "Reliability Analysis of Randomly Vibrating Structures With Parameter Uncertainties," J. Sound Vib., **297**, pp. 1000–1024.
[20] Manohar, C. S., and Gupta, S., 2004, "Seismic Probabilistic Safety Assessment of Nuclear Power Plant Structures," Project report, Indian Institute of Science, Bangalore, India.
[21] Nigam, N. C., and Narayanan, S., 1994, *Applications of Random Vibrations*, Narosa, New Delhi.
[22] Shinozuka, M., and Deodatis, G., 1996, "Simulation of Multidimensional Gaussian Stochastic Fields by Spectral Representation," Appl. Mech. Rev., **49**, pp. 29–53.
[23] Brodtkorb, P. A., Johannesson, P., Lingren, G., Rychlik, I., Rudén, J., and Sjö, E., 2000, "WAFO—A Matlab Toolbox for Analysis of Random Waves and Loads," *Proceedings of the tenth International Offshore and Polar Engineering Conference*, Vol. 3, pp. 343–350.
[24] Cramer, H., 1966, "On the Intersections Between Trajectories of a Normal Stationary Stochastic Process and a High Level," Arch. Math., **6**, pp. 337–349.
[25] Vanmarcke, E., 1972, "Properties of Spectral Moments With Applications to Random Vibrations," J. Engrg. Mech. Div., **98**, pp. 425–446.
[26] Rychlik, I., and Gupta, S., 2007, "Rain-Flow Fatigue Damage for Transformed Gaussian Loads," Int. J. Fatigue, **29**, pp. 406–420.
[27] Gupta, S., and Rychlik, I., 2007, "Rain-Flow Fatigue Damage Due to Nonlinear Combination of Vector Gaussian Loads," Probab. Eng. Mech., **22**, pp. 231–249.